



## Hong Kong vehicle emission changes from 2003 to 2015 in the Shing Mun Tunnel

Xiaoliang Wang, Kin-Fai Ho, Judith C. Chow, Steven D. Kohl, Chi Sing Chan, Long Cui, Shun-cheng Frank Lee, Lung-Wen Antony Chen, Steven Sai Hang Ho, Yan Cheng & John G. Watson

To cite this article: Xiaoliang Wang, Kin-Fai Ho, Judith C. Chow, Steven D. Kohl, Chi Sing Chan, Long Cui, Shun-cheng Frank Lee, Lung-Wen Antony Chen, Steven Sai Hang Ho, Yan Cheng & John G. Watson (2018) Hong Kong vehicle emission changes from 2003 to 2015 in the Shing Mun Tunnel, *Aerosol Science and Technology*, 52:10, 1085-1098, DOI: [10.1080/02786826.2018.1456650](https://doi.org/10.1080/02786826.2018.1456650)

To link to this article: <https://doi.org/10.1080/02786826.2018.1456650>

 View supplementary material [↗](#)

 Accepted author version posted online: 27 Mar 2018.  
Published online: 13 Apr 2018.

 Submit your article to this journal [↗](#)

 Article views: 103

 View Crossmark data [↗](#)

 Citing articles: 1 View citing articles [↗](#)



## Hong Kong vehicle emission changes from 2003 to 2015 in the Shing Mun Tunnel

Xiaoliang Wang<sup>a</sup>, Kin-Fai Ho<sup>b</sup>, Judith C. Chow<sup>a</sup>, Steven D. Kohl<sup>a</sup>, Chi Sing Chan<sup>b</sup>, Long Cui<sup>c</sup>, Shun-cheng Frank Lee<sup>c</sup>, Lung-Wen Antony Chen<sup>d</sup>, Steven Sai Hang Ho<sup>e,f</sup>, Yan Cheng<sup>g</sup>, and John G. Watson<sup>a</sup>

<sup>a</sup>Desert Research Institute, Reno, Nevada, USA; <sup>b</sup>The Chinese University of Hong Kong, Hong Kong, China; <sup>c</sup>Civil and Environmental Engineering, Hong Kong Polytechnic University, Hong Kong, China; <sup>d</sup>Environmental and Occupational Health, University of Nevada–Las Vegas, Las Vegas, Nevada, USA; <sup>e</sup>Hong Kong Premium Services and Research Laboratory, Hong Kong, China; <sup>f</sup>Institute of Earth Environment, Chinese Academy of Sciences, Xi'an, Shaanxi, China; <sup>g</sup>School of Human Settlements and Civil Engineering, Xi'an Jiaotong University, Xi'an, Shaanxi, China

### ABSTRACT

This study characterized motor vehicle emission rates and compositions in Hong Kong's Shing Mun tunnel (SMT) during 2015 and compared them to similar measurements from the same tunnel in 2003. Average PM<sub>2.5</sub> concentrations in the SMT decreased by ~70% from 229.1 ± 22.1 μg/m<sup>3</sup> in 2003 to 74.2 ± 2.1 μg/m<sup>3</sup> in 2015. Both PM<sub>2.5</sub> and sulfur dioxide (SO<sub>2</sub>) emission factors (EF<sub>D</sub>) were reduced by ~80% and total non-methane (NMHC) hydrocarbons EF<sub>D</sub> were reduced by 44%. These reductions are consistent with long-term trends of roadside ambient concentrations and emission inventory estimates, indicating the effectiveness of emission control measures. EF<sub>D</sub> changes between 2003 and 2015 were not statistically significant for carbon monoxide (CO), ammonia (NH<sub>3</sub>), and nitrogen oxides (NO<sub>x</sub>). Tunnel nitrogen dioxide (NO<sub>2</sub>) concentrations and NO<sub>2</sub>/NO<sub>x</sub> volume ratios increased, indicating an increased NO<sub>2</sub> fraction in the primary vehicle exhaust emissions. Elemental carbon (EC) and organic matter (OM) were the most abundant PM<sub>2.5</sub> constituents, with EC and OM, respectively, contributing to 51 and 31% of PM<sub>2.5</sub> in 2003, and 35 and 28% of PM<sub>2.5</sub> in 2015. Average EC and OM EF<sub>D</sub> decreased by ~80% from 2003 to 2015. The sulfate EF<sub>D</sub> decreased to a lesser degree (55%) and its contribution to PM<sub>2.5</sub> increased from 10% in 2003 to 18% in 2015, due to influences from ambient background sulfate concentrations. The contribution of geological materials to PM<sub>2.5</sub> increased from 2% in 2003 to 5% in 2015, signifying the importance of non-tailpipe emissions.

### ARTICLE HISTORY

Received 18 January 2018  
Accepted 18 March 2018

### EDITOR

Paul Ziemann

## 1. Introduction

Motor vehicles are a principal source of urban air pollution, directly emitting large amounts of carbon monoxide (CO), volatile organic compounds (VOC), nitrogen oxides (NO<sub>x</sub>), particulate matter (PM), and mobile source air toxics (Sawyer et al. 2000). Some of these pollutants react in the atmosphere to form secondary pollutants such as ozone (O<sub>3</sub>) and secondary inorganic/organic aerosols (Bahreini et al. 2012). Epidemiological and toxicological studies find that vehicle emissions contribute to a broad range of adverse health effects, such as allergies, asthma, other respiratory ailments, and cardiovascular disease (HEI 2010). Due to population and vehicle fleet growth as well as land use changes, more people are living and working close to busy highways and roads. The Health Effects Institute (HEI 2010) estimated that 30–45% of people in large North American cities live or work within an exposure zone of 300–500 m from busy

roads. Asian cities have higher human exposures to mobile source emissions owing to enclosed street canyons, near-road residences, and a high presence of people on sidewalks and roadways. In 2015, the road transport sector was estimated to contribute to 51% of CO, 18% of NO<sub>x</sub> and VOCs, and 10% of PM<sub>2.5</sub> primary emissions in Hong Kong (HKEPD 2017c). Transportation also contributed to 18, 26, and 25.5% of total greenhouse gas emissions in Hong Kong, the U.S., and European Union, respectively, most of which are from on-road mobile sources (EEA 2016; HKENB 2016; U.S. EPA 2016).

Concerns over health and climate effects have prompted worldwide efforts to reduce vehicle emissions, including advances in vehicle, engine, and after-treatment technologies, fuel improvements, traffic management optimization, and implementation of more stringent emission standards (HEI 2011; Shindell et al.

**CONTACT** Xiaoliang Wang ✉ [xiaoliang.wang@dri.edu](mailto:xiaoliang.wang@dri.edu) Desert Research Institute, 2215 Raggio Pkwy, Reno, NV 89512, USA.

Color versions of one or more of the figures in the article can be found online at [www.tandfonline.com/uast](http://www.tandfonline.com/uast).

Supplemental data for this article can be accessed on the [publisher's website](#).

2011). As shown in online supplementary information (SI) Table S1, Hong Kong has taken aggressive measures to reduce vehicle emissions, including replacing diesel fuel with liquefied petroleum gas (LPG) for almost all taxis and a large fraction of public light buses, reducing fuel sulfur content to 10 ppmw, and retrofitting older diesel vehicles with PM removal devices (HKEPD 2017a; Lau et al. 2015). These control measures have resulted in decreased roadside concentrations for sulfur dioxide (SO<sub>2</sub>) and PM<sub>2.5</sub> (Ai et al. 2016; HKEPD 2017a). However, due to population growth and increased goods shipment, daily vehicle-kilometers travelled (VKT) have steadily increased by 19% from 2003 to 2015 (HKTD 2016). VKT increases are even larger in developing nations due to rapid urbanization and motorization, partially offsetting emission reductions from vehicles. The chemical composition of vehicle emissions has also changed over time. For example, while diesel PM emissions show a decreasing trend, diesel engines with catalytic converters or particulate filters may increase tailpipe nitrogen dioxide (NO<sub>2</sub>) emissions (Tian et al. 2011; Wild et al. 2017). Enhanced emissions from gasoline and LPG vehicles in Hong Kong were found to increase the total non-methane hydrocarbon (NMHC) and O<sub>3</sub> concentrations from 2005 to 2013 (Lyu et al. 2017). Vehicle emissions were important contributors to elevated NO<sub>2</sub> and O<sub>3</sub> concentrations that exceeded the Hong Kong ambient air quality objectives (Ai et al. 2016).

Real-world characterizations of on-road vehicle fleet emissions over time (e.g., 10 years or more) are needed to evaluate emission changes, assess the effectiveness of emission control actions, and improve assessment of human exposure to vehicle emissions. Such measurements update current emission levels and serve as a baseline for future comparisons. Several methods have been used to characterize vehicle emissions, including chassis and engine dynamometer testing, remote sensing, on-road chasing, on-board measurements by portable emission measurement systems, and tunnel studies (Franco et al. 2013; HEI 2010). Among these methods, tunnel studies have several advantages: (1) the wind condition is well defined; (2) pollutant concentrations are dominated by vehicle-related tailpipe and non-tailpipe emissions; and (3) driving conditions represent the local real-world fuel, fleet, and operating conditions. Many tunnel studies have been conducted to evaluate the efficacy of control strategies and assess emission models (El-Fadel and Hashisho 2001; HEI 2010; Kuykendall et al. 2009).

This study examined vehicle emission changes over an 11-year interval through real-world emission characterizations in Hong Kong's Shing Mun tunnel (SMT). Similar measurements were conducted in summer and winter

of 2003 and repeated in 2015. Emission changes are compared to ambient concentrations and emission inventories to evaluate the effectiveness of emission control measures.

## 2. Experimental

### 2.1. Tunnel measurements

The SMT is a two-bore (north and south) tunnel on the HK Route 9 expressway connecting Sha Tin and Tsuen Wan urban areas in the New Territories (see map in the SI, Figure S1). The tunnel is 2.6 km long and divided into 1.6 km east and 1.0 km west sections. Each bore has two traffic lanes with 70 m<sup>2</sup> cross-sectional areas. There are 80 jet fans and four exhaust fans positioned along the tunnel ceiling which were not activated during this study. Ventilation was achieved by the piston effect of traffic movement. Daily vehicle flows were ~53,000 (HKTD 2016), with 2003/2015 average fleet mixes of ~41%/45% gasoline, ~9%/13% LPG, and ~50%/42% diesel-fueled vehicles.

Measurements from 2003 to 2015 were acquired in the south bore of the east section, which has a rising slope of 1.054% from the entrance to exit. Due to space and electricity constraints, the inlet and outlet sampling sites were placed 600 m apart, being 686 m from the entrance and 350 m from the exit, respectively, as shown in Figure 1a. The setback from the entrance minimized disturbances from outside air, and allowed pollutant concentrations to be homogenized across the tunnel cross-section (El-Fadel and Hashisho 2001). The posted speed limit was 80 km/h. Most vehicles were likely in hot-stabilized conditions as the closest highway ramp was ~2 km from the entrance.

Figure 1b shows the 2015 sampling system at the tunnel inlet and outlet with greater detail shown in Figure S2 of the SI. Instrument specifications are listed in Table S2 of the SI. Gas and particle samples were drawn from inlets located at 1.5 m above ground level adjacent to the right traffic lane. CO, CO<sub>2</sub>, nitric oxide (NO), NO<sub>2</sub>, and SO<sub>2</sub> were measured with near real-time gas analyzers. A DustTrak DRX (Wang et al. 2009), a micro-aethalometer, and a condensation particle counter acquired continuous PM mass, black carbon (BC), and particle number concentration, respectively. Two collocated DRI 13-channel medium-volume multichannel sampling system (Chow et al. 1993) collected filter samples for laboratory analyses. Three parallel channels were activated during each sampling period, including: (1) a Teflon-membrane filter backed by a citric acid-impregnated cellulosic-fiber filter, (2) a quartz-fiber filter, and (3) a quartz-fiber filter backed by a quartz-fiber filter.

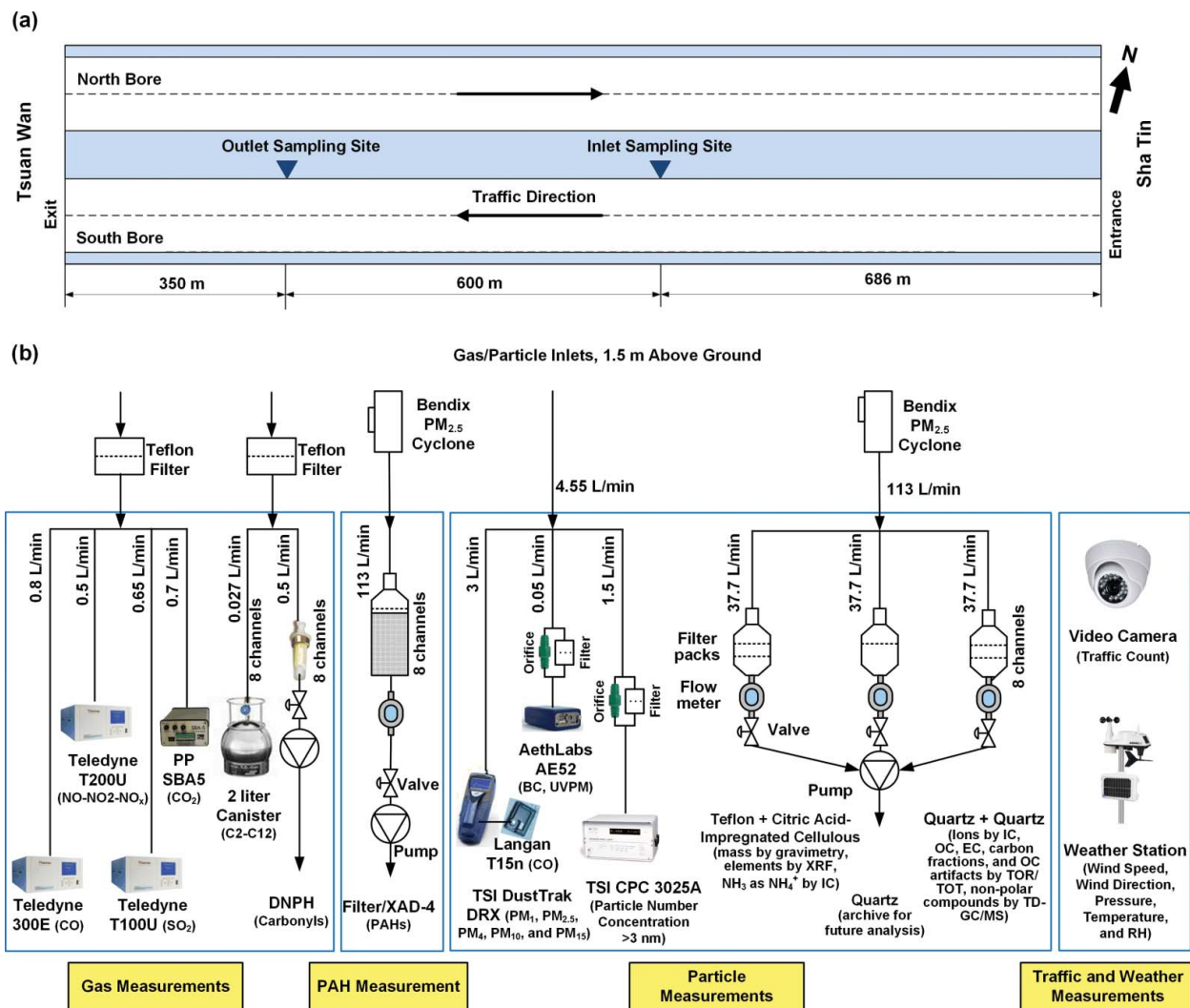


**Figure 1.** Schematic diagram of: (a) west section sample configuration of the Shing Mun Tunnel (SMT) in Hong Kong and (b) sampling setup at the outlet site of the SMT in 2015.

Each sampler automatically sequenced through the 12 channels (with one passive channel for the field blank) and acquired eight sets of samples without operator intervention. NMHCs were collected in canisters for off-line analyses by gas chromatography–mass spectrometry (Cui et al. 2018). Additional measurements for carbonyls and polycyclic aromatic hydrocarbons will be reported in future publications. Two video cameras recorded the traffic flow at the tunnel entrance and the outlet sampling site. Wind speeds, wind directions, barometric pressures (P), temperatures (T), and relative humidities (RH) were monitored by weather stations at both inlet and outlet sites. Real-time instruments were calibrated before, during, and/or after the field campaign. Linear regressions were performed between the instrument reading and calibration standards, and the regression equations were used to adjust the raw instrument readings. Gas analyzers with different manufacturers or model numbers were used in the 2003 study, but were

calibrated with the same standard gases with known concentrations (Cheng et al. 2006).

Sampling was conducted from 1/19/2015 to 3/15/2015 with a recess during the Chinese New Year (2/16/2015–3/1/2015). Continuous CO<sub>2</sub> and PM monitors, meteorological stations, and traffic cameras were operated continuously over the ~2-month period. Filter sampling was conducted four days per week with sample changes in early mornings (~midnight to 0500 local standard time [LST]) on Mondays and Wednesdays when the south bore was closed for maintenance. For each sampling day, four 2-h sampling periods were chosen to capture the morning and evening rush hours (0800–1000 and 1700–1900 LST) when diesel vehicle proportions were the lowest and midday hours (1100–1300 and 1400–1600 LST) when diesel vehicle proportions were the highest. A total of 66 filter pairs (both inlet and outlet) were collected with 53 on weekdays and 13 on weekends. Near real-time gas and particle data were acquired

continuously, but data analysis excluded periods when either tunnel bore was closed for maintenance.

The SMT toll booths recorded hourly counts of vehicles in light-, medium-, and heavy-duty (LD, MD, and HD, respectively) categories, but these data do not separate taxis (fueled by LPG) from other gasoline-powered LD vehicles. Manual traffic counting from the tunnel entrance videos separated the fleet into nine categories (i.e., motorcycle, private car, taxi, light goods vehicle, medium goods vehicle, heavy goods vehicle, light bus, single deck bus, and double deck bus) with a time resolution of 15 min for each 2-h sampling period. Total vehicle numbers differed by <4% between manual counting and toll booth records.

## 2.2. Laboratory analysis and quality assurance

Teflon-membrane filters were analyzed for PM<sub>2.5</sub> mass by gravimetry (Watson et al. 2017) and 51 elements (sodium through uranium) by X-ray fluorescence (XRF) (Watson et al. 1999). To minimize mass uncertainty due to particle-bound water at high ambient RH, filters were equilibrated in a controlled environment with 21.5 ± 1.5°C temperature and 35 ± 5% RH for at least 24 h before weighing. Half of the quartz-fiber filters were extracted in distilled-deionized water and analyzed for six water-soluble ions (i.e., chloride [Cl<sup>-</sup>], nitrate [NO<sub>3</sub><sup>-</sup>], sulfate [SO<sub>4</sub><sup>2-</sup>], ammonium [NH<sub>4</sub><sup>+</sup>], sodium [Na<sup>+</sup>], and potassium [K<sup>+</sup>]) by ion chromatography (IC; Chow and Watson 2017). A 0.5 cm<sup>2</sup> punch of the quartz-fiber filter was analyzed for organic carbon (OC), elemental carbon (EC), and eight thermal fractions following the IMPROVE\_A thermal/optical protocol (Chow et al. 2007). The backup citric acid-impregnated cellulose-fiber filter was extracted and analyzed for NH<sub>3</sub> as NH<sub>4</sub><sup>+</sup> by automated colorimetry (AC), and the backup quartz-fiber filter was analyzed by the IMPROVE\_A protocol to estimate the organic vapors adsorbed onto the front quartz-fiber filter (Chow et al. 2010; Watson et al. 2009).

Physical consistency was evaluated for: (1) sum of measured species versus gravimetric mass; (2) reconstructed mass versus gravimetric mass; (3) SO<sub>4</sub><sup>2-</sup> versus elemental sulfur (S); (4) water-soluble potassium (K<sup>+</sup>) versus total K; (5) calculated versus measured NH<sub>4</sub><sup>+</sup>; and (6) anion and cation balance. The sum of PM<sub>2.5</sub> chemical species should be less than or equal to the corresponding gravimetric PM mass, since unmeasured species such as oxygen (O) and hydrogen (H) were not included. Figure S3 a of the SI shows good correlation (correlation coefficient  $r = 0.91$ ) between sum of species and gravimetric mass, with a slope of 0.85, an intercept of 3.78 μg/m<sup>3</sup>, and an average ratio of 0.93 ± 0.16. PM

mass reconstruction applies a set of coefficients to measured species and estimate unmeasured components (Chow et al. 2015). Figure S3b of the SI shows that the reconstructed and measured PM<sub>2.5</sub> mass was correlated ( $r = 0.89$ ) with a slope (0.89) closer to unity than that of the sum of species (0.85). The average ratio between reconstructed and gravimetric mass was 1.01 ± 0.18, indicating valid measurements for major PM<sub>2.5</sub> components.

SO<sub>4</sub><sup>2-</sup> was measured by IC using quartz-fiber filter extracts while elemental S was measured by XRF on Teflon-membrane filters. Within precision estimates, the molar ratio of S to SO<sub>4</sub><sup>2-</sup> is expected to equal one if all S exists as water-soluble SO<sub>4</sub><sup>2-</sup> and greater than one due to the presence of water-insoluble and/or organic S. Figure S3c of the SI shows that most samples were on or below the 1:1 line with a few exceptions. Possible causes of higher SO<sub>4</sub><sup>2-</sup> than S molar concentrations are: (1) volatile sulfur-containing species (e.g., H<sub>2</sub>SO<sub>4</sub>) were measured by IC, but were vaporized under the vacuum and higher temperature environment of the XRF analysis chamber; and (2) the filters were heavily loaded and the X-ray may not totally penetrate the particle layer, causing underestimation of S. The IC SO<sub>4</sub><sup>2-</sup> measurement is a more accurate measurement for both cases. Water-soluble K<sup>+</sup> measured by IC on the quartz-fiber filter extracts should be equal to or less than total K measured by XRF on the Teflon-membrane filter. Figure S3d of the SI shows a K<sup>+</sup>/K slope of 0.58 with a low (-0.10 μg/m<sup>3</sup>) intercept, indicating that soluble K<sup>+</sup> was always less than the total K as expected.

NH<sub>4</sub><sup>+</sup> is commonly found in the chemical forms of ammonium nitrate (NH<sub>4</sub>NO<sub>3</sub>), ammonium sulfate [(NH<sub>4</sub>)<sub>2</sub>SO<sub>4</sub>], and ammonium bisulfate (NH<sub>4</sub>HSO<sub>4</sub>). Ammonium chloride (NH<sub>4</sub>Cl) concentration may be found near salt lakebeds or areas with deicing material, but their concentrations are generally low and not included in the calculation. The measured NH<sub>4</sub><sup>+</sup> can be compared with calculated NH<sub>4</sub><sup>+</sup> assuming full [(NH<sub>4</sub>)<sub>2</sub>SO<sub>4</sub>] or partial (NH<sub>4</sub>HSO<sub>4</sub>) neutralization. Figure S3e of the SI shows that the calculated and measured NH<sub>4</sub><sup>+</sup> had high correlations ( $r > 0.98$ ), and the slope between calculated NH<sub>4</sub><sup>+</sup> assuming the sum of NH<sub>4</sub>NO<sub>3</sub> and (NH<sub>4</sub>)<sub>2</sub>SO<sub>4</sub> was 1.05, indicating that the NH<sub>4</sub><sup>+</sup> was fully neutralized as NH<sub>4</sub>NO<sub>3</sub> and (NH<sub>4</sub>)<sub>2</sub>SO<sub>4</sub>. Figure S3f of the SI shows an excellent balance between the measured anions and cations with a slope of 0.99 and  $r$  of 1.00, indicating particles were nearly neutral and adequate ions were measured.

## 2.3. Emission factor calculation

Real-time data were transformed to 1-min averages, and time series were inspected to identify outliers or

instrument malfunction. The 1-min data were further averaged over the 2-h sampling periods of integrated samples. Distance-based emission factors ( $EF_D$ ; in g/veh/km) were calculated based on the mass balance principle (El-Fadel and Hashisho 2001; Gertler et al. 2002; Pierson et al. 1996). Considering the tunnel section bounded by the inlet and outlet sampling sites and assuming that pollutants do not deposit or react within this section, the mass of the pollutant  $i$  ( $Mass_i$ ; in g) produced by vehicles within the tunnel section during a sampling period  $\Delta t$  (in s) can be calculated as:

$$Mass_i = (C_{i,out}U_{out} - C_{i,in}U_{in}) A \Delta t \quad [1]$$

where  $C_{i,in}$  and  $C_{i,out}$  are the average concentrations (g/m<sup>3</sup>) of pollutant  $i$  measured at the inlet and outlet sampling sites, respectively, and  $U_{in}$  and  $U_{out}$  are the wind speed (m/s) at the inlet and outlet, respectively,  $A$  (m<sup>2</sup>) is the tunnel cross-section area, and  $\Delta t$  (s) is sampling period. The  $EF_{D,i}$  for species  $i$  is then:

$$EF_{D,i} = Mass_i / NL \quad [2]$$

where  $N$  is the number of vehicles through the tunnel section during the sampling period and  $L$  (m) is the length of the tunnel section between the inlet and outlet sampling sites.  $EF_D$  are usually reported for on-road vehicle emissions and are comparable with vehicle emission standards and mobile source emission models. In contrast, power- or carbon-based emission factors are often used for nonroad engines (Wang et al. 2016).

Several recent studies used roadside in-plume sampling and fast-response ( $\leq 1$  s) instruments to determine carbon-based emission factors from individual vehicles, particularly from high emitters (Dallmann et al. 2012; Wang et al. 2015). This method requires a stable background so that the short-duration (5–20 s) concentration peaks by individual vehicles are clearly discernable. It was found that the concentrations inside the busy SMT were too variable to establish a stable baseline to calculate individual vehicle emission factors. Therefore, fleet average  $EF_D$  are reported here.

### 3. Results

#### 3.1. Temporal patterns of traffic, gases, and particles

Figure 2 illustrates the diurnal variations of traffic counts (i.e., LD, MD, and HD), gaseous (i.e., CO, SO<sub>2</sub>, NO, NO<sub>2</sub>), and PM (i.e., PM<sub>2.5</sub> and PM<sub>10</sub>) concentrations measured at the outlet site. Additional diurnal pattern of tunnel ambient T, RH, wind speed, and CO<sub>2</sub> concentration are shown in Figure S4 of the SI. Because the traffic

patterns were different, data are presented in groups of weekdays and weekends. Figure S5 of the SI depicts an example of continuous data measured on 26 January 2015.

Figure 2a shows two traffic peaks around 0800 and 1800 LST on weekdays for LD vehicles (including motorcycles, private cars, and taxis), corresponding to morning and afternoon rush hours, respectively. Traffic flows for MD vehicles (including light- and medium-duty trucks and light buses) and HD vehicles (including heavy duty trucks, and single and double deck buses) were relatively uniform during the daytime (~0800–1800 LST) and lower during early mornings and evenings. Traffic counts from videos show an average of 50% gasoline, 14% LPG, and 36% diesel vehicles during morning (0800–1000 LST) and afternoon (1700–1900 LST) rush hours on weekdays. The vehicle fleet contained 37% gasoline, 12% LPG, and 51% diesel vehicles during midday sampling periods (1100–1300 and 1400–1600 LST).

Traffic patterns were different on weekends (Figure 2b). LD vehicle counts gradually increased in the daytime and peaked around 1800 LST with a second peak around 2100–2200 LST, indicating increased late-night activities. While the total LD vehicles counts were similar between weekdays and weekends, the total number of MD and HD vehicles was 30–40% lower on weekends. The gasoline vehicle fraction increased from 46% during 0800–1000 LST to 61% during 1700–1900 LST, LPG fraction remained at 15–20% throughout the day, while diesel vehicle fractions were 30–35% during the day and 24% during 1700–1900 LST on weekends.

Pearson correlation coefficients ( $r$ ) in Table 1 show that CO<sub>2</sub>, NO, NO<sub>2</sub>, SO<sub>2</sub>, PM<sub>2.5</sub>, and PM<sub>10</sub> were highly correlated ( $r > 0.96$ ) with lower correlations ( $r = 0.57$ – $0.71$ ) between CO and other pollutants. Diurnal patterns of CO concentrations (Figures 2c and d) were similar to the LD vehicle counts (Figures 2a and b) with  $r = 0.91$  for LD as compared to  $r = 0.53$  for MD and HD. CO is expected to be better correlated with LD because spark-ignition LD engines emit higher CO (Kean et al. 2003) than compression-ignition MD and HD diesel engines. On the other hand, NO, NO<sub>2</sub>, SO<sub>2</sub>, and PM concentrations had higher correlations with MD and HD ( $r > 0.94$ ) than LD ( $r \leq 0.90$ ), consistent with MD and HD being larger NO<sub>x</sub>, SO<sub>2</sub>, and PM emitters. As illustrated in Figure S5 of the SI, BC also showed diurnal patterns similar to MD and HD traffic counts. CO<sub>2</sub> concentrations (Figures S4e and f, SI) may be influenced by both the larger number of LD vehicles with lower  $EF_D$  and the lower number of MD and HD vehicles with higher  $EF_D$ . Therefore, CO<sub>2</sub> diurnal variations had mixed contributions from all vehicle categories and the  $r$  values (0.92–0.94) were similar among vehicle categories.

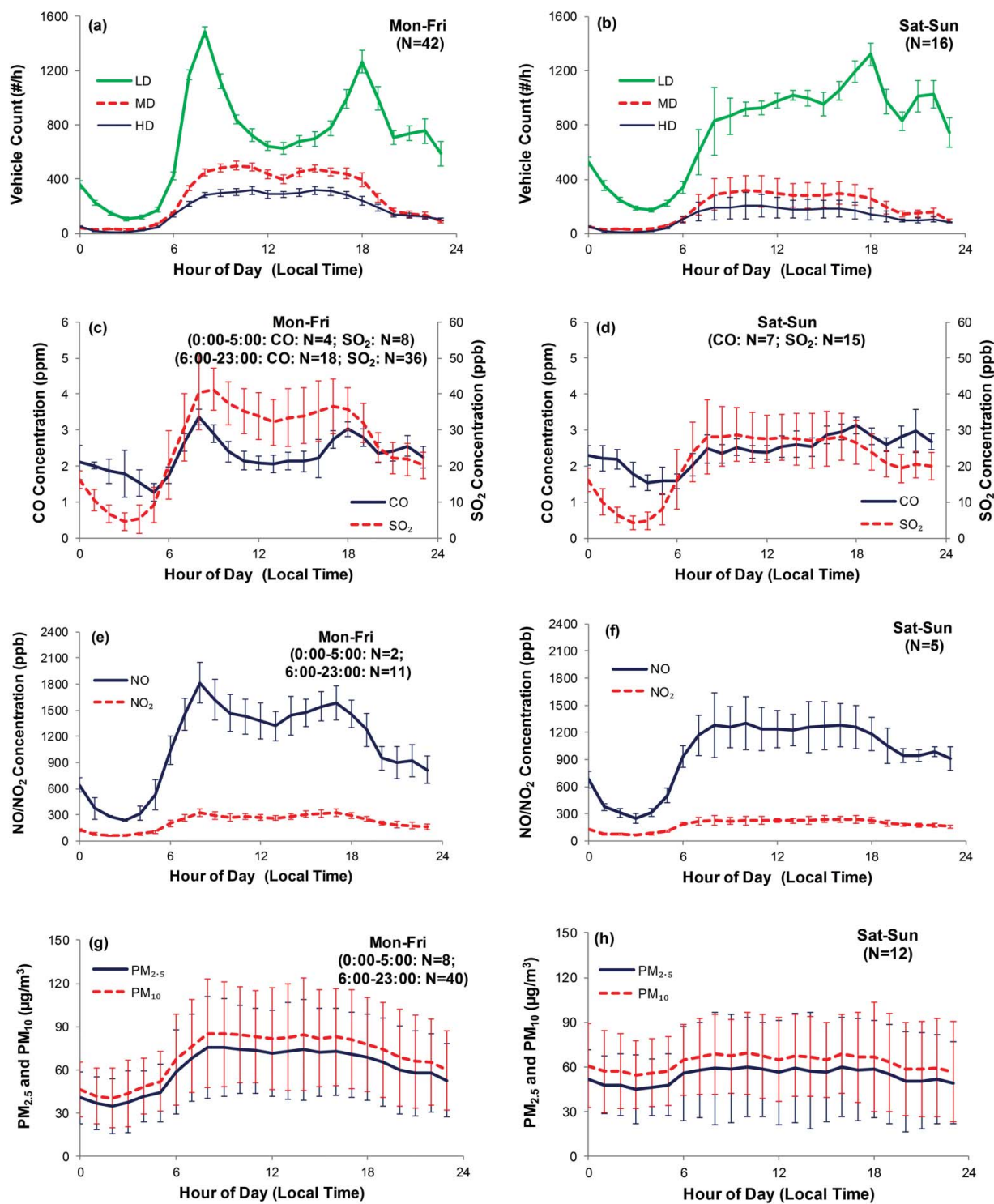


**Figure 2.** Diurnal variations (hourly average) of SMT outlet measurements: westbound traffic count of light-duty (LD), medium-duty (MD), and heavy-duty (HD) vehicles (a and b); CO and SO<sub>2</sub> concentrations (c and d); NO and NO<sub>2</sub> concentrations (e and f); and DRX PM<sub>2.5</sub> and PM<sub>10</sub> concentrations normalized by gravimetric mass (g and h) during weekdays (left panels) and weekends (right panels). Error bars represent the standard deviation of the hourly average data, and N represents the number of days for which the indicated measurement is available. Because one of the bores was closed for cleaning and maintenance during 0000–0500 LST on Monday–Thursday and all traffic was redirected to the other bore, only Friday data was averaged for 0000–0500 LST to represent weekdays.

**Table 1.** Pearson correlation coefficients ( $r$ ) among pollutant concentrations and vehicle categories<sup>a</sup>.

Parameter	CO <sub>2</sub>	CO	NO	NO <sub>2</sub>	SO <sub>2</sub>	PM <sub>2.5</sub>	PM <sub>10</sub>	LD	MD	HD
CO <sub>2</sub>	1.00	0.76	0.99	0.98	0.99	0.97	0.96	0.94	0.92	0.94
CO	0.76	1.00	0.67	0.64	0.71	0.59	0.57	0.91	0.53	0.53
NO	0.99	0.67	1.00	0.99	0.99	0.98	0.98	0.89	0.94	0.96
NO <sub>2</sub>	0.98	0.64	0.99	1.00	0.98	0.98	0.98	0.87	0.95	0.97
SO <sub>2</sub>	0.99	0.71	0.99	0.98	1.00	0.98	0.97	0.90	0.94	0.96
PM <sub>2.5</sub>	0.97	0.59	0.98	0.98	0.98	1.00	1.00	0.83	0.97	0.99
PM <sub>10</sub>	0.96	0.57	0.98	0.98	0.97	1.00	1.00	0.81	0.98	0.99
LD	0.94	<b>0.91</b>	<b>0.89</b>	<b>0.87</b>	<b>0.90</b>	<b>0.83</b>	<b>0.81</b>	1.00	0.77	0.77
MD	0.92	<b>0.53</b>	<b>0.94</b>	<b>0.95</b>	<b>0.94</b>	<b>0.97</b>	<b>0.98</b>	0.77	1.00	0.99
HD	0.94	<b>0.53</b>	<b>0.96</b>	<b>0.97</b>	<b>0.96</b>	<b>0.99</b>	<b>0.99</b>	0.77	0.99	1.00

<sup>a</sup>Correlation coefficients between pollutant concentration and vehicle categories with  $r > 0.9$  are in bold and  $r \leq 0.9$  are in bold italic.

### 3.2. Concentrations and emission factors of gases and particles

Table 2 compares inlet and outlet concentrations as well as fleet-average EF<sub>D</sub> between 2003 (Cheng et al. 2006; HKPolyU 2005; Ho et al. 2009) and 2015. The 2015 EF<sub>D</sub> values (average  $\pm$  standard error) are: 301.80  $\pm$  6.31 g/veh/km for CO<sub>2</sub>, 1.80  $\pm$  0.13 g/veh/km for CO, 0.059  $\pm$  0.002 g/veh/km for total measured NMHCs, 0.019  $\pm$  0.001 g/veh/km for NH<sub>3</sub>, 0.87  $\pm$  0.08 g/veh/km for NO, 0.24  $\pm$  0.02 g/veh/km for NO<sub>2</sub>, 1.58  $\pm$  0.14 g/veh/km for NO<sub>x</sub> (as NO<sub>2</sub>), 0.047  $\pm$  0.002 g/veh/km for SO<sub>2</sub>, and 0.025  $\pm$  0.003 g/veh/km for PM<sub>2.5</sub>.

The most significant decreases are found for SO<sub>2</sub> and PM<sub>2.5</sub>, with  $\sim$ 80% reduction in EF<sub>D</sub> from 2003 to 2015. These reductions are likely due to emission controls, such as reducing the fuel sulfur content (50 to 10 ppmw for diesel and 150 to 10 ppmw for gasoline), retrofitting diesel particulate filters (DPF) or diesel oxidation catalysts (DOC), and changing a large fraction of public light buses (PLBs) from diesel to LPG fuels (Table S1, SI). EF<sub>D</sub> for total measured NMHCs decreased by 44% from 2003 to 2015. Cui et al. (2018) show that most NMHC species decreased between the two studies. For example, ethene and propene (key markers for diesel emissions) EF<sub>D</sub> decreased by  $\sim$ 65% from 2003 to 2015, indicating effective pollution control. However, *i*-butane and *n*-butane, markers for LPG emissions, increased by 32 and 17%, respectively. Note that while  $\sim$ 93% of PLBs were powered by diesel in 2003,  $\sim$ 70% of PLBs were powered by LPG in 2015. Correspondingly, the fraction of LPG vehicles increased from 9 to 13% from 2003 to 2015. The total LPG consumption by the transportation sector increased by 26% from 2003 to 2015 (HKEMSD 2017). EF<sub>D</sub> for CO<sub>2</sub>, CO, NO, and NO<sub>x</sub> in 2015 were 3%, 5%, 11%, and 8% lower than those in 2003, respectively. However, the differences were not statistically significant at  $p < 0.05$  based on Student's *t*-test. EF<sub>D</sub> for NO<sub>2</sub> and NH<sub>3</sub> were somewhat higher in 2015 than in 2003.

Table 2 shows that most pollutant concentrations decreased from 2003 to 2015, indicating improved tunnel

air quality and reduced vehicle emissions. Despite the 20–30% NO and NO<sub>x</sub> concentration decrease, NO<sub>2</sub> concentrations in 2015 were 1.4 and 2.2 times those in 2003 at the SMT inlet and outlet, respectively, consistent with the nondecreasing trend of ambient NO<sub>2</sub> concentrations in Hong Kong (HKEPD 2017a). The 2015 NO<sub>2</sub>/NO<sub>x</sub> volume ratios at the SMT inlet and outlet were 16.6  $\pm$  2.2% and 16.3  $\pm$  1.6%, respectively, while the corresponding ratios were 5.8  $\pm$  2.7% and 9.5  $\pm$  2.0%, respectively, in 2003, indicating an increased NO<sub>2</sub> fraction in primary exhaust emissions. These increases are probably related to a higher number of vehicles with DOCs, which catalytically convert NO to NO<sub>2</sub> for oxidizing CO, hydrocarbons, and PM (Millstein and Harley 2010; Tian et al. 2011). Similar trends have been observed in other cities (Carslaw et al. 2011).

Table S3 of the SI compares fleet average EF<sub>D</sub> measured from several tunnels since 2000. EF<sub>D</sub> vary among studies owing to variations in fleet compositions, fuel, road gradients, and environmental parameters. The Zhujiang tunnel in Guangzhou, China ( $\sim$ 130 km northwest of SMT) has a fleet composition and geographical location similar to those of the SMT (Liu et al. 2014; Zhang et al. 2015). Ratios of the fleet averaged EF<sub>D</sub> between SMT (2015) and Zhujiang tunnel (2014) were 0.77 for CO<sub>2</sub>, 0.58 for CO, 0.13 for NMHCs, 0.08 for NH<sub>3</sub>, 0.84 for NO<sub>x</sub>, and 0.30 for PM<sub>2.5</sub>. The exception is for SO<sub>2</sub> (with unknown reason), where SMT was 2.2 times the EF<sub>D</sub> in the Zhujiang tunnel. The lower EF<sub>D</sub> for most species in the SMT is likely due to the more aggressive emission controls in Hong Kong compared to those in mainland China. The gasoline and diesel sulfur content was 10 ppmw in Hong Kong during the 2015 measurement, while the fuel sulfur content was 50 ppmw in Guangzhou during the 2014 measurement.

Brimblecombe et al. (2015) characterized vehicle emissions from three tunnels in Hong Kong using a mobile platform driving through the tunnels in 2014. The carbon-based emission factors (EF<sub>C</sub>; in g/kg<sup>-C</sup>) from SMT and these three tunnels are compared in Table S4. The EF<sub>C</sub> for CO in SMT (22.5  $\pm$  0.6 g/kg<sup>-C</sup>) was within

**Table 2.** Comparison of SMT inlet and outlet concentrations and fleet average emission factors (EF<sub>D</sub>) for gases and PM<sub>2.5</sub> between 2003 and 2015. Values are expressed as average ± standard error.

Species <sup>a</sup>	SMT 2003			SMT 2015			EF <sub>D</sub> Ratio (2015/2003)	Statistical Significance (p-value)
	Concentration		EF <sub>D</sub> (g/veh/km)	Concentration		EF <sub>D</sub> (g/veh/km)		
	Inlet	Outlet		Inlet	Outlet			
CO <sub>2</sub> (ppm)	580.0 ± 10.4	710.0 ± 16.7	310.00 ± 16.89	645.3 ± 20.7	788.7 ± 23.6	301.80 ± 6.31	0.97	0.65
CO (ppm)	2.7 ± 0.2	4.2 ± 0.3	1.88 ± 0.11	1.3 ± 0.1	2.6 ± 0.1	1.80 ± 0.13	0.95	0.61
NMHCs (ppb)	73.6 ± 1.5	107.6 ± 2.2	0.106 ± 0.002	42.7 ± 0.9	60.8 ± 1.2	0.059 ± 0.002	0.56	0.00
NH <sub>3</sub> (μg/m <sup>3</sup> )	NA <sup>b</sup>	22.9 ± 6.9	0.017 ± 0.003	25.7 ± 1.7	41.9 ± 2.7	0.019 ± 0.001	1.16	0.41
NO (ppb)	1358.7 ± 74.8	1923.8 ± 109.2	0.98 ± 0.08	952.7 ± 45.6	1475.1 ± 117.1	0.87 ± 0.08	0.89	0.32
NO <sub>2</sub> (ppb)	87.2 ± 9.0	198.7 ± 12.4	0.22 ± 0.03	189.4 ± 9.7	285.9 ± 22.7	0.24 ± 0.02	1.11	0.51
NO <sub>x</sub> (ppb)	1445.9 ± 81.6	2118.4 ± 117.4	1.72 ± 0.13	1142.1 ± 31.9	1761.0 ± 49.9	1.58 ± 0.14	0.92	0.44
SO <sub>2</sub> (ppb)	20.6 ± 8.3	83.7 ± 6.6	0.208 ± 0.016	20.8 ± 1.0	36.3 ± 1.7	0.047 ± 0.002	0.23	0.00
PM <sub>2.5</sub> (μg/m <sup>3</sup> )	172.7 ± 11.3	285.4 ± 22.3	0.131 ± 0.037	62.1 ± 3.5	83.1 ± 4.5	0.025 ± 0.003	0.19	0.01

<sup>a</sup>The units in the Species column are for concentrations of each species.

<sup>b</sup>The inlet NH<sub>3</sub> was not measured in 2003 and data from a nearby ambient monitoring station was used for EF<sub>D</sub> calculation. Therefore, the 2003 NH<sub>3</sub> data is listed for information only.

the range of Aberdeen Tunnel (ABT; 26.2 g/kg<sup>-C</sup>), Lion Rock Tunnel (LRT; 15.8 g/kg<sup>-C</sup>), and Tai Lam Tunnel (TLT; 13.0 g/kg<sup>-C</sup>). The higher EF<sub>c</sub> for CO in ABT was likely due to its higher LPG vehicle fraction (26%) than the other tunnels (6–13%). The EF<sub>c</sub> for NO<sub>x</sub> in SMT (20.5 ± 0.9 g/kg<sup>-C</sup>) was also within the range of ABT (19.3 g/kg<sup>-C</sup>), LRT (26.7 g/kg<sup>-C</sup>), and TLT (28.5 g/kg<sup>-C</sup>). The higher EF<sub>c</sub> for NO<sub>x</sub> in TLT was likely due to its higher diesel vehicle fraction (46%) than other tunnels (33–42%). The EF<sub>c</sub> for PM<sub>2.5</sub> in SMT in 2015 was 49–73% of those reported for the other three tunnels. The PM<sub>2.5</sub> in ABT, LRT, and TLT was measured by a DustTrak, which overestimates ambient PM<sub>2.5</sub> gravimetric mass by about a factor of two using default calibration factors (Wang et al. 2009). Therefore, the EF<sub>c</sub> for PM<sub>2.5</sub> in SMT were likely within the range of the other three tunnels after accounting for the DustTrak calibration. The EF<sub>c</sub> for BC in ABT, LRT and TLT were 5–7 times higher than the EC measured in SMT, and were also higher than the EF<sub>c</sub> for PM<sub>2.5</sub> in the same tunnels by a factor of two. BC was measured by an Aethalometer AE33, which is known to deviate from EC due to artifacts such as filter matrix and particle loading effects (Collaud Coen et al. 2015).

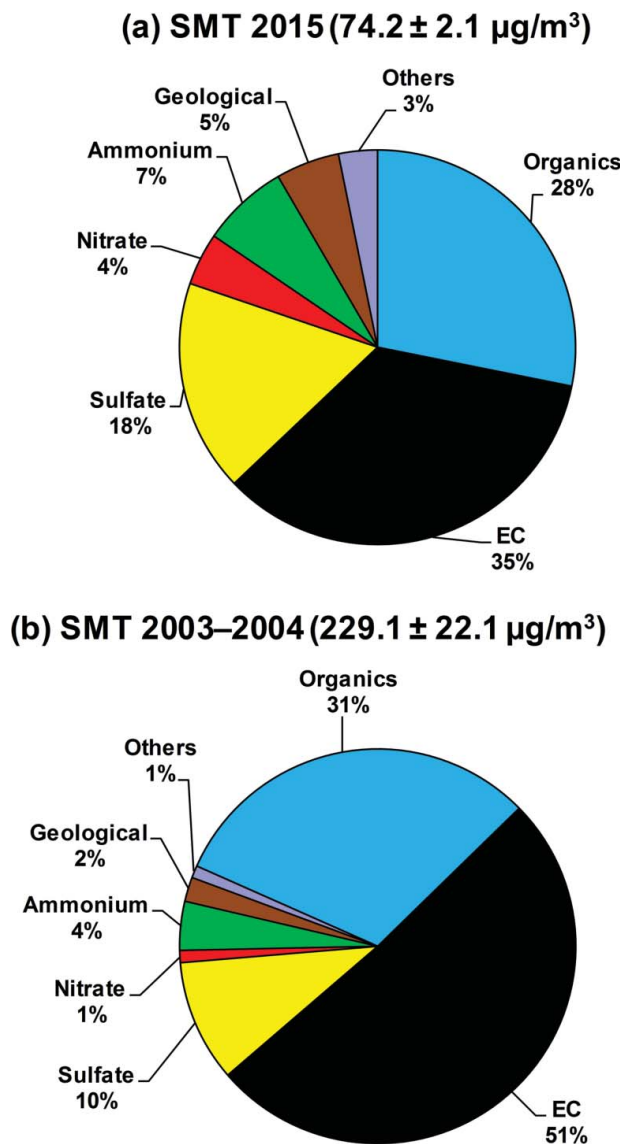
### 3.3. Concentration and emission factors of PM<sub>2.5</sub> constituents

Figure 3 shows the reconstructed PM<sub>2.5</sub> mass (Chow et al. 2015) assuming major constituents of organic matter (OM = OC × 1.2), EC, SO<sub>4</sub><sup>2-</sup>, NO<sub>3</sub><sup>-</sup>, NH<sub>4</sub><sup>+</sup>, geological materials (estimated as 2.2 × [Al] + 2.49 × [Si] + 1.63 × [Ca] + 1.94 × [Ti] + 2.42 × [Fe]), and others (i.e., other measured ions, elements, and unidentified species). The largest abundance differences between 2003 and 2015 are found for EC and SO<sub>4</sub><sup>2-</sup>. Figure 4 compares the 2015 and

2003 EF<sub>D</sub> for PM<sub>2.5</sub> elements, ions, and carbon. Detailed concentration and EF<sub>D</sub> values are listed in Table S5 (SI). EF<sub>D</sub> for almost all species showed significant decrease, contributing to overall decrease of PM<sub>2.5</sub> emissions.

The average PM<sub>2.5</sub> concentration decreased by ~70% from 229.1 ± 22.1 μg/m<sup>3</sup> in 2003 to 74.2 ± 2.1 μg/m<sup>3</sup> in 2015. While the OM abundance remained similar (~30%), the EC fraction in PM<sub>2.5</sub> decreased from 51% in 2003 to 35% in 2015. The OC/EC ratio was 0.7 ± 0.2 in 2015, similar to that in 2003 (0.5 ± 0.2). The largest decrease of ~80% is found for EC, from 114.1 ± 10.0 μg/m<sup>3</sup> in 2003 to 24.8 ± 0.8 μg/m<sup>3</sup> in 2015. A corresponding reduction of 77% is found in EF<sub>D</sub> for EC from 65.8 ± 18.4 mg/veh/km in 2003 to 15.0 ± 1.2 mg/veh/km in 2015. Similarly, average OM concentrations decreased by ~70% from 70.2 ± 7.6 μg/m<sup>3</sup> in 2003 to 20.3 ± 0.8 μg/m<sup>3</sup> in 2015, and the corresponding EF<sub>D</sub> was reduced by 78% from 42.8 ± 14.0 to 9.3 ± 1.4 mg/veh/km. LPG vehicles emit little primary PM and the LPG markers showed increased emissions; therefore, the OM reduction is not likely due to LPG emission changes and is attributable to gasoline and diesel emission improvements.

The SO<sub>4</sub><sup>2-</sup> concentration in the SMT decreased by 48%, from 23.7 ± 9.3 μg/m<sup>3</sup> in 2003 to 12.3 ± 5.2 μg/m<sup>3</sup> in 2015. The SO<sub>4</sub><sup>2-</sup> in the SMT represents a combination of vehicle emissions and the ambient background. The ambient SO<sub>4</sub><sup>2-</sup> concentrations also decreased 42–47% from 2003 to 2015 (HKEPD 2017d), owing to aggressive SO<sub>2</sub> emission controls, such as reducing sulfur content in industrial and vehicle fuels, retrofitting power plants with flue gas desulfurization devices, and regulating boat emissions near shore. Figure 5 compares SO<sub>4</sub><sup>2-</sup> concentrations at the SMT inlet and outlet sites to those obtained from two nearby (<5 km) ambient air monitoring sites (Kwai Chuang and Tsuen Wan). The similar tunnel and ambient concentrations suggest that the ambient background



**Figure 3.** Comparison of reconstructed  $\text{PM}_{2.5}$  mass with species measured at the SMT from: (a) 2015 and (b) 2003 for samples collected from both inlet and outlet sites. OM = organic carbon  $\times 1.2$ ; geological material =  $2.2 \times [\text{Al}] + 2.49 \times [\text{Si}] + 1.63 \times [\text{Ca}] + 1.94 \times [\text{Ti}] + 2.42 \times [\text{Fe}]$  (Chow et al. 2015).

dominated the tunnel  $\text{SO}_4^{2-}$  concentrations. Due to the significant reductions in EC and OC, the sulfate abundance in the SMT  $\text{PM}_{2.5}$  was higher in 2015 (18%) than that in 2003 (10%). The  $\text{NH}_4^+$  concentration in the SMT decreased by 39%, from  $8.3 \pm 3.1 \mu\text{g}/\text{m}^3$  in 2003 to  $5.1 \pm 2.6 \mu\text{g}/\text{m}^3$  in 2015, similar to a 35–41% decrease in ambient concentrations. Although the ambient  $\text{NO}_3^-$  concentrations also decreased by 33–50%, the tunnel  $\text{NO}_3^-$  concentrations were comparable between 2003 ( $3.1 \pm 2.5 \mu\text{g}/\text{m}^3$ ) and 2015 ( $3.4 \pm 3.8 \mu\text{g}/\text{m}^3$ ). Both  $\text{NH}_4^+$  and  $\text{NO}_3^-$  concentrations in the SMT were about 15–25% higher than those measured at the nearby ambient monitoring sites, indicating the dominance of ambient background influences.

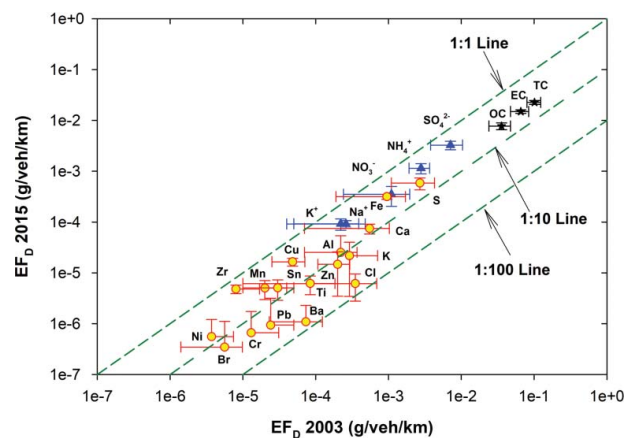


**Figure 4.** Comparison of  $\text{PM}_{2.5}$  elements (circle), ions (triangle), and carbon (star) emission rates measured in 2003 and 2015. Error bars represent standard error of the mean.

Geological mineral concentrations were similar during the two studies:  $4.3 \pm 0.8 \mu\text{g}/\text{m}^3$  in 2003 and  $4.0 \pm 0.4 \mu\text{g}/\text{m}^3$  in 2015. Due to the decrease in SMT  $\text{PM}_{2.5}$  concentrations, the abundance of geological materials increased from 2% in 2003 to 5% in 2015. Geological materials largely originate from non-tailpipe emissions, e.g., road dust, tire wear, and brake wear. The increased geological fraction confirms the trend that non-tailpipe emissions become more important in traffic-related emissions as tailpipe emissions decrease (Amato et al. 2014; Denier van der Gon et al. 2013).

#### 3.4. Comparison with emission inventory and ambient concentrations

Figure 6 examines emission inventory and roadside ambient concentration trends in Hong Kong. More details of the annual average ambient concentrations at

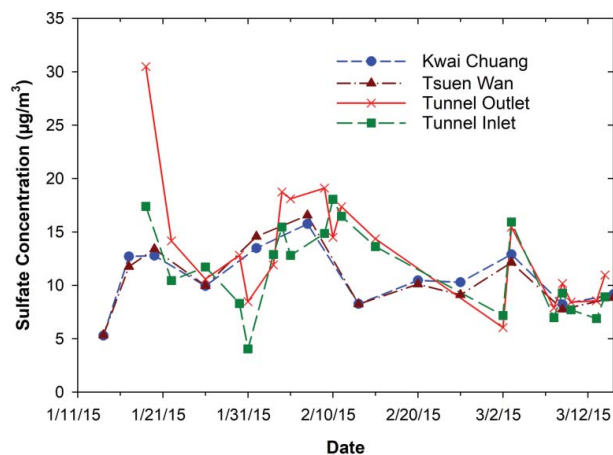


**Figure 5.** Sulfate concentrations measured at the inlet and outlet of the SMT and two ambient monitoring stations near the SMT during the 2015 tunnel measurement period.

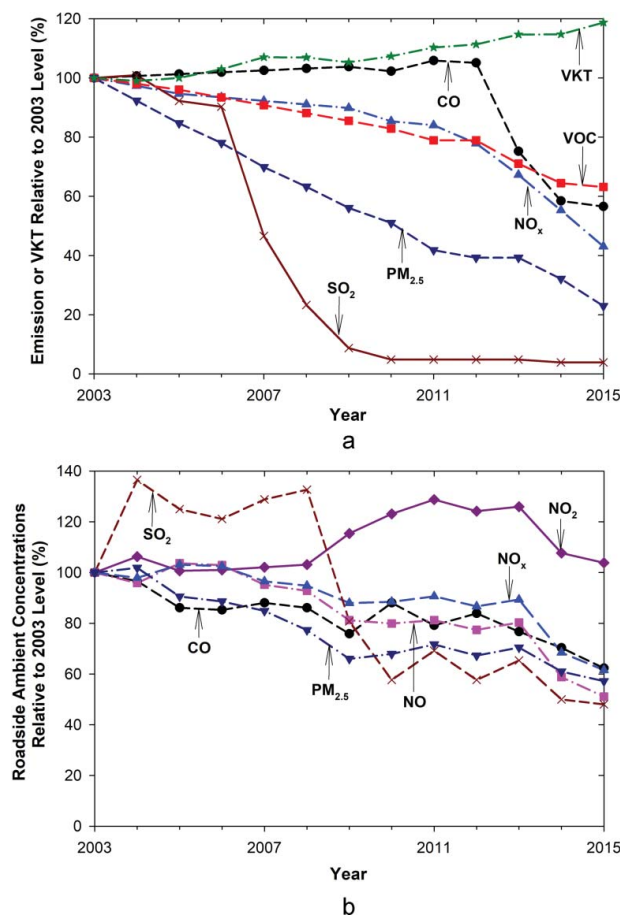


**Figure 6.** Trends of: (a) estimate of criteria pollutant emissions by the road transport sector and vehicle kilometer travelled (VKT) in Hong Kong relative to 2003 level (HKEPD 2017c; HKTD 2016); and (b) ambient concentrations measured from roadside sites in Hong Kong. The y-axis shows levels normalized by 2003 values.

roadside (heavy traffic streets surrounded by many tall buildings), urban, new town (mainly residential), and rural land use sites are plotted in Figure S6 of the SI.

Despite a 19% increase in VKT from 2003 to 2015, both emission inventory and roadside concentrations showed decreasing trends for most criteria pollutants. As shown in Table 3, the 2015/2003 emission inventory ratios were 0.57 for CO, 0.43 for NO<sub>x</sub>, 0.04 for SO<sub>2</sub>, 0.63 for total VOCs, and 0.23 for PM<sub>2.5</sub>. The 2015/2003 roadside concentration ratios were 0.62 for CO, 0.51 for NO, 1.04 for NO<sub>2</sub>, 0.62 for NO<sub>x</sub>, 0.48 for SO<sub>2</sub>, and 0.57 for PM<sub>2.5</sub>. Note that the comparison in Table 3 is qualitative because the tunnel emissions only represent vehicles in hot-stabilized conditions at speeds of ~80 km/h, while traffic patterns on city streets are more diverse, including cold and hot starts, stop and go, and transient conditions. Furthermore, the vehicle fleet compositions in the tunnel differ from the Hong Kong-averaged fleet compositions. While the average gasoline, LPG, and diesel vehicles were ~45, 13, and 42% in SMT during 2015, the corresponding

**Table 3.** Comparison of 2015/2003 ratios for gases and PM<sub>2.5</sub> in Hong Kong among emission rates in SMT, road transport emission inventory, and roadside ambient concentrations.

Data source	Ratio of 2015 to 2003 Level						
	CO	NO	NO <sub>2</sub>	NO <sub>x</sub>	SO <sub>2</sub>	VOCs	PM <sub>2.5</sub>
Emission Estimates based on Tunnel Studies <sup>a</sup>	1.13	1.06	1.32	1.09	0.27	0.61	0.23
Road Transport Emission Inventory	0.57	NA	NA	0.43	0.04	0.63	0.23
Roadside Concentration	0.62	0.51	1.04	0.62	0.48	NA	0.57

<sup>a</sup>Emissions were calculated by multiplying 2015/2003 ratios of EF<sub>D</sub> (Table 2) with VKT (1.19).

average VKT fractions were 42, 24, and 34%, respectively, in Hong Kong as a whole (HKEPD 2017b).

For CO, while the emission inventory shows a slight increasing trend from 2003 to 2011 and then a sharp drop from 2012 to 2015 (Figure 6a), roadside concentrations show a decreasing trend from 2003 to 2015 (Figure 6b). The ~40% reductions in inventory and roadside concentrations were not observed in the SMT measurements. While the fleet average EF<sub>D</sub> (1.88 and 1.80 g/veh/km) were similar between 2003 and 2015 (Table 2), the estimated CO emission from tunnel studies increased by 13% (Table 3). Figure S6a shows that urban CO concentrations increased by ~23% while new town residential area and rural CO concentrations decreased by 20–30% from 2003 to 2015.

While NO and NO<sub>x</sub> inventory emissions and roadside concentrations decreased by 40–60%, tunnel-measured NO and NO<sub>x</sub> emissions increased by 6–9%. The reasons why tunnel fleet average EF<sub>D</sub> for CO, NO, and NO<sub>x</sub> did not decrease as much as emission inventory or roadside ambient concentrations are not clear. As mentioned earlier, different driving conditions between SMT and city streets as well as the 3–8% higher diesel and gasoline vehicle fractions in the SMT could be the contributing factors. While tunnel-measured NO<sub>2</sub> emissions increased by 32% from 2003 to 2015, roadside concentrations only increased by 4%. Figure S6c shows that roadside NO<sub>2</sub> concentrations increased during 2008–2011, which was partially attributed to malfunctioning catalytic converters on LPG vehicles (Lyu et al. 2016). The replacement of LPG catalytic converters in 2013–2014 effectively reduced roadside NO, NO<sub>2</sub>, and NO<sub>x</sub> concentrations (Figures S6b–d, SI) as well as VOC emissions (Figure 6a), according to the emission inventory.

Tunnel emission estimates, emission inventory, and roadside concentrations all showed large decreases for SO<sub>2</sub> and PM<sub>2.5</sub>. Both emissions and roadside SO<sub>2</sub> concentrations (Figure 6) stayed at low levels since 2010 when sulfur contents in gasoline and diesel were reduced to 10 ppmw.

The substantial decreases in CO, NO<sub>x</sub>, SO<sub>2</sub>, VOC, and PM<sub>2.5</sub> emissions and roadside concentrations from 2003

to 2015 could be attributed to an array of vehicle emission control programs (Table S1, SI). For example, a sharp decrease in roadside  $\text{SO}_2$  concentrations was observed between 2008 and 2010, coinciding with the adoption of the Euro V motor fuel (10 ppmw S) standard from 2007. Efforts have been made to reduce diesel emissions, such as retrofitting DPF, DOC, and selective catalytic reduction devices on older diesel vehicles, phasing in Euro IV standard in 2006 and Euro V in 2010, and retiring 47% of the pre-Euro IV diesel commercial vehicles by 2015 (HKEPD 2017a,c). The effectiveness of these efforts is evident from the significant reductions in  $\text{PM}_{2.5}$ , EC, ethene, and propene emissions observed in this study.

#### 4. Discussion and conclusions

This study characterized real-world gas and particle emissions from on-road vehicles in the SMT in Hong Kong. The temporal patterns of traffic and pollutant concentrations were examined to illustrate the correlations between fleet components and pollutants. SMT traffic patterns on weekdays showed clear morning and afternoon rush hour peaks for LD vehicles, while weekend LD vehicles counts gradually increased throughout the day and peaked in the evening. MD and HD vehicle counts were higher in daytime than evenings. CO concentration variations showed better correlation with the LD than MD or HD vehicle counts, while NO,  $\text{NO}_2$ ,  $\text{SO}_2$ , and PM concentrations had higher correlations with MD and HD than LD.

The 2015 fleet-average  $\text{EF}_D$  values (average  $\pm$  standard error) are:  $301.80 \pm 6.31$  g/veh/km for  $\text{CO}_2$ ,  $1.80 \pm 0.13$  g/veh/km for CO,  $0.059 \pm 0.002$  g/veh/km for total NMHCs,  $0.019 \pm 0.001$  g/veh/km for  $\text{NH}_3$ ,  $0.87 \pm 0.08$  g/veh/km for NO,  $0.24 \pm 0.02$  g/veh/km for  $\text{NO}_2$ ,  $1.58 \pm 0.14$  g/veh/km for  $\text{NO}_x$  (as  $\text{NO}_2$ ),  $0.047 \pm 0.002$  g/veh/km for  $\text{SO}_2$ , and  $0.025 \pm 0.003$  g/veh/km for  $\text{PM}_{2.5}$ . These values provide useful information about current emission levels and serve as a baseline for future comparisons. However, these values were obtained under specific conditions: fleet composition ( $\sim 45\%$  gasoline,  $\sim 13\%$  LPG, and  $\sim 42\%$  diesel) with vehicles under hot-stabilized operations at  $\sim 80$  km/h; near flat road gradient (1.054% uphill); and stable ambient temperature ( $\sim 20$ – $25^\circ\text{C}$ ) and RH ( $\sim 60$ – $70\%$ ). These well-defined conditions will be used for evaluating vehicle emission models, such as the Emission FACTors-Hong Kong (EMFAC-HK). Several earlier tunnel studies used linear regression methods to apportion the fleet-average emission factors to different traffic components, such as LD versus HD or gasoline versus diesel (Cheng et al. 2006; Gertler et al. 2002; Pierson et al. 1996). However, the

correlations between 2-h average  $\text{EF}_D$  and diesel vehicle fraction were found to be poor in this study. For example, as shown in Figure S7 of the SI, the coefficient of determination ( $R^2$ ) was only 0.10 between  $\text{NO}_x$   $\text{EF}_D$  and diesel vehicle fraction, preventing a reliable apportionment using the linear regression method. Instead, a weight-of-evidence approach employing the positive matrix factorization solution to the chemical mass balance equations, temporal pattern of traffic and pollutant concentrations, and chemical source profiles of VOCs and  $\text{PM}_{2.5}$  was used to derive emission factors and estimate contributions from gasoline, LPG, and diesel vehicles. The EMFAC-HK evaluation and source apportionment will be reported in future publications.

The comparison of emissions between the 2003 and 2015 tunnel measurements allows examination of vehicle emission factor and emission composition changes. The tunnel emissions were further compared to emission inventory and ambient concentrations to evaluate the effectiveness of emission control measures. From 2003 to 2015, the  $\text{EF}_D$  for  $\text{SO}_2$  and  $\text{SO}_4^{2-}$  decreased by  $\sim 80$  and 55%, respectively. These reductions can be attributed to aggressive  $\text{SO}_2$  emission reductions from industry, vehicles, marine transport, and power plants in Hong Kong and nearby regions.  $\text{EF}_D$  for  $\text{PM}_{2.5}$ , EC, and OM were reduced by  $\sim 80\%$  from 2003 to 2015. Since diesel vehicles have higher  $\text{EF}_D$  for  $\text{PM}_{2.5}$  and EC, their significant reduction indicates the controls for reducing diesel emissions were effective (e.g., retrofitting emission control devices on older diesel vehicles, phasing in vehicles with newer emission standards, phasing out older vehicles, and changing some light buses from diesel to LPG). The effectiveness of diesel emission controls are also evident from the reduction of NMHC markers for diesel emissions (e.g., ethene and propene  $\text{EF}_D$  decreased by  $\sim 65\%$  from 2003 to 2015). The reduction of OM and total NMHC also indicates that gasoline emissions were also reduced. However, due to the increased number of LPG vehicles and LPG consumption,  $\text{EF}_D$  for i-butane and n-butane, markers for LPG emissions, increased by 32 and 17%, respectively.

From 2003 to 2015, inventoried emissions and roadside concentrations showed 40–60% decrease for CO, NO, and  $\text{NO}_x$ , contrary to the 6–13% increase from the tunnel measurements. The reasons for these discrepancies warrant further investigation.  $\text{NO}_2$  emissions estimated from tunnel measurements increased by 32% from 2003 to 2015, qualitatively consistent with the non-decreasing trend in ambient  $\text{NO}_2$  concentrations. The  $\text{NO}_2/\text{NO}_x$  volume ratios at the SMT inlet and outlet increased from  $5.8 \pm 2.7\%$  and  $9.5 \pm 2.0\%$  in 2003, to  $16.6 \pm 2.2\%$  and  $16.3 \pm 1.6\%$  in 2015, respectively, indicating an increased  $\text{NO}_2$  fraction in primary vehicle exhaust emissions.

EC, OM, and  $\text{SO}_4^{2-}$  were the largest contributors to  $\text{PM}_{2.5}$  mass in both tunnel studies. While the EC and OM fractions decreased due to vehicle emission controls, the contribution of  $\text{SO}_4^{2-}$  increased, owing to the larger influence of ambient background  $\text{SO}_4^{2-}$  concentrations. The geological material concentrations remained similar between the two tunnel studies, while their abundances in  $\text{PM}_{2.5}$  mass increased from 2% in 2003 to 5% in 2015. As tailpipe emissions are being aggressively regulated and reduced, non-tailpipe emissions (e.g., road dust, tire wear, and brake wear) are becoming more important.

## Acknowledgments

The authors are grateful to the Hong Kong Environmental Protection Department and Hong Kong Transport Department for provision of the data sets and permission for sampling in the SMT. The content of this article does not necessarily reflect the views and policies of the Hong Kong Special Administrative Region Government, nor does the mention of trade names or commercial products constitute endorsement or recommendation of use.

The investigators are thankful for the helpful operational and technical advice from Drs. Maria Costantini, Johanna Boogaard, Allison Patton, and other HEI staff. We are grateful to the teams in The Chinese University of Hong Kong, The Hong Kong Polytechnic University, and DRI for field sampling, chemical analysis, traffic counting, and data analysis. The contents of this article do not necessarily reflect the views of HEI or its sponsors, nor do they necessarily reflect the views and policies of the EPA or motor vehicle and engine manufacturers.

## Funding

This research was supported by the Health Effects Institute (HEI; Grant 4947-RFPA14-1/15-1), an organization jointly funded by the United States Environmental Protection Agency (EPA) (Assistance Award No. R-82811201) and certain motor vehicle and engine manufacturers. This research was also partially supported by the Research Grants Council (RGC) of Hong Kong Government (PolyU 152090/15E) and the Hong Kong RGC Collaborative Research Fund (C5022-14G).

## References

- Ai, Z.T., Mak, C.M., Lee, H.C. (2016). Roadside air quality and implications for control measures: A case study of Hong Kong. *Atmos. Environ.*, 137:6–16.
- Amato, F., Cassee, F.R., Denier van der Gon, H.A.C., Gehrig, R., Gustafsson, M., Hafner, W., Harrison, R.M., Jozwicka, M., Kelly, F.J., Moreno, T., Prevot, A.S.H., Schaap, M., Sunyer, J., Querol, X. (2014). Urban air quality: The challenge of traffic non-exhaust emissions. *J. Hazard. Mater.*, 275 (0):31–36.
- Bahreini, R., Middlebrook, A.M., de Gouw, J.A., Warneke, C., Trainer, M., Brock, C.A., Stark, H., Brown, S.S., Dube, W.P., Gilman, J.B., Hall, K., Holloway, J.S., Kuster, W.C., Perring, A.E., Prevot, A.S.H., Schwarz, J.P., Spackman, J.R., Szidat, S., Wagner, N.L., Weber, R.J., Zotter, P., Parrish, D.D. (2012). Gasoline emissions dominate over diesel in formation of secondary organic aerosol mass. *Geophys. Res. Lett.*, 39 (6):L06805.
- Brimblecombe, P., Townsend, T., Lau, C.F., Rakowska, A., Chan, T.L., Močnik, G., Ning Z. (2015). Through-tunnel estimates of vehicle fleet emission factors. *Atmos. Environ.*, 123, Part A:180–189.
- Carslaw, D.C., Beevers, S.D., Tate, J.E., Westmoreland, E.J., Williams, M.L. (2011). Recent evidence concerning higher  $\text{NO}_x$  emissions from passenger cars and light duty vehicles. *Atmos. Environ.*, 45 (39):7053–7063.
- Cheng, Y., Lee, S.C., Ho, K.F., Louie, P.K.K. (2006). On-road particulate matter ( $\text{PM}_{2.5}$ ) and gaseous emissions in the Shing Mun Tunnel, Hong Kong. *Atmos. Environ.*, 40 (23):4235–4245.
- Cheng, Y., Lee, S.C., Ho, K.F., Chow, J.C., Watson, J.G., Louie, P.K.K., Cao, J.J., Hai, X. (2010). Chemically-specified on-road  $\text{PM}_{2.5}$  motor vehicle emission factors in Hong Kong. *Sci. Total Environ.*, 408 (7):1621–1627.
- Chow, J.C., Watson, J.G., Bowen, J.L., Frazier, C.A., Gertler, A. W., Fung, K.K., Landis, D., Ashbaugh, L.L. (1993). A sampling system for reactive species in the western United States, in: *Sampling and Analysis of Airborne Pollutants*, Winegar, E.D., Keith, L.H. (Eds.). Lewis Publishers, Ann Arbor, MI, pp. 209–228.
- Chow, J.C., Watson, J.G., Chen, L.-W.A., Chang, M.C.O., Robinson, N.F., Trimble, D., Kohl, S. (2007). The IMPROVE\_A temperature protocol for thermal/optical carbon analysis: maintaining consistency with a long-term database. *J. Air Waste Manage. Assoc.*, 57 (9):1014–1023.
- Chow, J.C., Watson, J.G., Chen, L.-W.A., Rice, J., Frank, N.H. (2010). Quantification of  $\text{PM}_{2.5}$  organic carbon sampling artifacts in US networks. *Atmos. Chem. Phys.*, 10 (12):5223–5239.
- Chow, J.C., Lowenthal, D.H., Chen, L.W.A., Wang, X.L., Watson, J.G. (2015). Mass reconstruction methods for  $\text{PM}_{2.5}$ : a review. *Air Qual. Atmos. Health*, 8 (3):243–263.
- Chow, J.C., Watson, J.G. (2017). Enhanced ion chromatographic speciation of water-soluble  $\text{PM}_{2.5}$  to improve aerosol source apportionment. *Aerosol Sci. Eng.*, 1:7–24.
- Collaud Coen M., Weingartner E., Apituley A., Ceburnis D., Fierz-Schmidhauser R., Flentje H., Henzing J.S., Jennings S. G., Moerman M., Petzold A., Schmid O., Baltensperger U. (2010). Minimizing light absorption measurement artifacts of the aethalometer: Evaluation of five correction algorithms. *Atmos. Meas. Tech.* 3:457–474.
- Cui, L., Wang, X.L., Ho, K.F., Gao, Y., Liu, C., Ho, S.S., Li, H., Lee, S.C., Wang, X., Jiang, B., Huang, Y., Chow, J.C., Watson, J.G., Chen, L.-W.A. (2018). Decrease of VOC emissions from vehicular emissions in Hong Kong from 2003 to 2015: results from a tunnel study. *Atmos. Environ.*, 177:64–74.
- Dallmann, T.R., DeMartini, S.J., Kirchstetter, T.W., Herndon, S.C., Onasch, T.B., Wood, E.C., Harley, R.A. (2012). On-road measurement of gas and particle phase pollutant emission factors for individual heavy-duty diesel trucks. *Environ. Sci. Technol.*, 46 (15):8511–8518.
- Denier van der Gon, H.A.C., Gerlofs-Nijland, M.E., Gehrig, R., Gustafsson, M., Janssen, N., Harrison, R.M., Hulskotte, J.,

- Johansson, C., Jozwicka, M., Keuken, M., Krijgsheld, K., Ntziachristos, L., Riediker, M., Cassee, F.R. (2013). The policy relevance of wear emissions from road transport, now and in the future — an international workshop report and consensus statement. *J. Air Waste Manage. Assoc.*, 63 (2):136–149.
- EEA. (2016). *Greenhouse gas emissions from transport*. IND-111-en, European Environment Agency, Copenhagen, Denmark. Accessed on 3/8/2017. <http://www.eea.europa.eu/data-and-maps/indicators/transport-emissions-of-greenhouse-gases/transport-emissions-of-greenhouse-gases-6>
- El-Fadel, M., Hashisho, Z. (2001). Vehicular emissions in roadway tunnels: a critical review. *Crit. Rev. Environ. Sci. Technol.*, 31 (2):125–174.
- Franco, V., Kousoulidou, M., Muntean, M., Ntziachristos, L., Hausberger, S., Dilara, P. (2013). Road vehicle emission factors development: A review. *Atmos. Environ.*, 70:84–97.
- Gertler, A.W., Gillies, J.A., Pierson, W.R., Rogers, C.F., Sagebiel, J.C., Abu-Allaban, M., Coulombe, W., Tarnay, L., Cahill, T.A. (2002). *Real-World Particulate Matter and Gaseous Emissions from Motor Vehicles in a Highway Tunnel-HEI Research Report Number 107*. Health Effects Institute, Boston MA. Accessed on 10/10/2014. <http://pubs.healtheffects.org/getfile.php?u=171>
- HEI. (2010). *Traffic-Related Air Pollution: A Critical Review of the Literature on Emissions, Exposure, and Health Effects. HEI Special Report 17*. Health Effects Institute Panel on the Health Effects of Traffic-Related Air Pollution, Boston MA. Accessed on 8/5/2014. <http://pubs.healtheffects.org/getfile.php?u=553>
- HEI. (2011). *The Future of Vehicle Fuels and Technologies: Anticipating Health Benefits and Challenges. HEI Communication 16*. Health Effects Institute Special Committee on Emerging Technologies, Boston MA. Accessed on 8/5/2014. <http://pubs.healtheffects.org/getfile.php?u=635>
- HKEMSD. (2017). *Hong Kong Energy End-use Data 2017*. Hong Kong Electrical & Mechanical Services Department (EMSD), Hong Kong. Accessed on 12/14/2017. [https://www.emsd.gov.hk/filemanager/en/content\\_762/HKKEUD2017.pdf](https://www.emsd.gov.hk/filemanager/en/content_762/HKKEUD2017.pdf)
- HKENB. (2016). *Greenhouse Gas Emissions in Hong Kong by Sector*. Environment Bureau of the Government of the Hong Kong Special Administrative Region Hong Kong. Accessed on 7/1/2017. [https://www.climateready.gov.hk/files/pdf/HKGGHG\\_Sectors\\_201612.pdf](https://www.climateready.gov.hk/files/pdf/HKGGHG_Sectors_201612.pdf)
- HKEPD. (2017a). *Cleaning the Air at Street Level*. Hong Kong Environmental Protection Department. Accessed on 7/2/2017. [www.epd.gov.hk/epd/english/environmentinhk/air/prob\\_solutions/cleaning\\_air\\_atroad.html](http://www.epd.gov.hk/epd/english/environmentinhk/air/prob_solutions/cleaning_air_atroad.html)
- HKEPD. (2017b). *EMFAC-HK Vehicle Emission Calculation (Version 3.3)*. Hong Kong Environmental Protection Department.
- HKEPD. (2017c). *Hong Kong Air Pollutant Emission Inventory*. Environmental Protection Department, The Government of the Hong Kong Special Administrative Region, Hong Kong. Accessed on 4/10/2017. [http://www.epd.gov.hk/epd/english/environmentinhk/air/data/emission\\_inve.html](http://www.epd.gov.hk/epd/english/environmentinhk/air/data/emission_inve.html)
- HKEPD. (2017d). *Hong Kong Air Quality Monitoring Data*. Environmental Protection Department, The Government of the Hong Kong Special Administrative Region, Hong Kong. Accessed on 3/10/2017. [http://epic.epd.gov.hk/EPI\\_CDI/air/station/?lang=en](http://epic.epd.gov.hk/EPI_CDI/air/station/?lang=en)
- HKPolyU. (2005). *Determination of suspended particulate & VOC emission profiles for vehicular sources in Hong Kong*. Hong Kong Environmental Protection Department. Hong Kong Polytechnic University, Hong Kong, SAR. [http://www.epd.gov.hk/epd/english/environmentinhk/air/study/rpts/files/1-pt\\_final\\_report\\_20050225d.pdf](http://www.epd.gov.hk/epd/english/environmentinhk/air/study/rpts/files/1-pt_final_report_20050225d.pdf)
- HKTD. (2016). *The Annual traffic Census 2015*. TTSD Publication No. 16CAB1, Hong Kong Transport Department, Traffic and Transport Survey Division. [http://www.td.gov.hk/filemanager/en/content\\_4772/annual%20traffic%20census%202015.pdf](http://www.td.gov.hk/filemanager/en/content_4772/annual%20traffic%20census%202015.pdf)
- Ho, K.F., Lee, S.C., Ho, W.K., Blake, D.R., Cheng, Y., Li, Y.S., Ho, S.S.H., Fung, K., Louie, P.K.K., Park, D. (2009). Vehicular emission of volatile organic compounds (VOCs) from a tunnel study in Hong Kong. *Atmos. Chem. Phys.*, 9 (19):7491–7504.
- Kean, A.J., Harley, R.A., Kendall, G.R. (2003). Effects of vehicle speed and engine load on motor vehicle emissions. *Environ. Sci. Technol.*, 37 (17):3739–3746.
- Kuykendall, J.R., Shaw, S.L., Paustenbach, D., Fehling, K., Kacew, S., Kabay, V. (2009). Chemicals present in automobile traffic tunnels and the possible community health hazards: A review of the literature. *Inhalation Toxicol.*, 21 (9):747–792.
- Lau, C.F., Rakowska, A., Townsend, T., Brimblecombe, P., Chan, T.L., Yam, Y.S., Močnik, G., Ning, Z. (2015). Evaluation of diesel fleet emissions and control policies from plume chasing measurements of on-road vehicles. *Atmos. Environ.*, 122:171–182.
- Liu, T., Wang, X., Wang, B., Ding, X., Deng, W., Lü, S., Zhang, Y. (2014). Emission factor of ammonia (NH<sub>3</sub>) from on-road vehicles in China: tunnel tests in urban Guangzhou. *Environ. Res. Lett.*, 9 (6):064027.
- Lyu, X.P., Guo, H., Simpson, I.J., Meinardi, S., Louie, P.K.K., Ling, Z., Wang, Y., Liu, M., Luk, C.W.Y., Wang, N., Blake, D.R. (2016). Effectiveness of replacing catalytic converters in LPG-fueled vehicles in Hong Kong. *Atmos. Chem. Phys.*, 16 (10):6609–6626.
- Lyu, X.P., Zeng, L.W., Guo, H., Simpson, I.J., Ling, Z.H., Wang, Y., Murray, F., Louie, P.K.K., Saunders, S.M., Lam, S.H.M., Blake, D.R. (2017). Evaluation of the effectiveness of air pollution control measures in Hong Kong. *Environ. Pollut.*, 220:87–94.
- Millstein, D.E., Harley, R.A. (2010). Effects of retrofitting emission control systems on in-use heavy diesel vehicles. *Environ. Sci. Technol.*, 44 (13):5042–5048.
- Pierson, W.R., Gertler, A.W., Robinson, N.F., Sagebiel, J.C., Zielinska, B., Bishop, G.A., Stedman, D.H., Zweidinger, R.B., Ray, W.D. (1996). Real-world automotive emissions — Summary of studies in the Fort McHenry and Tuscarora mountain tunnels. *Atmos. Environ.*, 30 (12):2233–2256.
- Sawyer, R.F., Harley, R.A., Cadle, S.H., Norbeck, J.M., Slott, R., Bravo, H.A. (2000). Mobile sources critical review: 1998 NARSTO assessment. *Atmos. Environ.*, 34 (12–14):2161–2181.
- Shindell, D., Faluvegi, G., Walsh, M., Anenberg, S.C., Van Dingenen, R., Muller, N.Z., Austin, J., Koch, D., Milly, G. (2011). Climate, health, agricultural and economic impacts of tighter vehicle-emission standards. *Nature Clim. Change*, 1 (1):59–66.

- Tian, L., Hossain, S., Lin, H., Ho, K., Lee, S., Yu, I.S. (2011). Increasing trend of primary NO<sub>2</sub> exhaust emission fraction in Hong Kong. *Environ. Geochem. Health*, 33 (6):623–630.
- U.S. EPA. (2016). *Fast Facts - US Transportation Sector Greenhouse Gas Emissions: 1990–2014*. EPA-420-F-13-033a, Office of Transportation and Air Quality, U.S. Environmental Protection Agency Accessed on 3/8/2017. <https://www.epa.gov/green-vehicles/fast-facts-transportation-greenhouse-gas-emissions>
- Wang, J.M., Jeong, C.H., Zimmerman, N., Healy, R.M., Wang, D.K., Ke, F., Evans, G.J. (2015). Plume-based analysis of vehicle fleet air pollutant emissions and the contribution from high emitters. *Atmos. Meas. Tech.*, 8 (8):3263–3275.
- Wang, X.L., Chancellor, G., Evenstad, J., Farnsworth, J.E., Hase, A., Olson, G.M., Sreenath, A., Agarwal, J.K. (2009). A novel optical instrument for estimating size segregated aerosol mass concentration in real time. *Aerosol Sci. Technol.*, 43 (9):939–950.
- Wang, X.L., Chow, J.C., Kohl, S.D., Percy, K.E., Legge, A.H., Watson, J.G. (2016). Real-world emission factors for Caterpillar 797B heavy haulers during mining operations. *Particulology*, 28:22–30.
- Watson, J.G., Chow, J.C., Frazier, C.A. (1999). X-ray fluorescence analysis of ambient air samples, in: *Elemental Analysis of Airborne Particles*, Vol. 1. Landsberger, S., Creatchman, M. (Eds.), Gordon and Breach Science, Amsterdam, The Netherlands, pp. 67–96.
- Watson, J.G., Chow, J.C., Chen, L.-W.A., Frank, N.H. (2009). Methods to assess carbonaceous aerosol sampling artifacts for IMPROVE and other long-term networks. *J. Air Waste Manage. Assoc.*, 59 (8):898–911.
- Watson, J.G., Tropp, R.J., Kohl, S.D., Wang, X.L., Chow, J.C. (2017). Filter processing and gravimetric analysis for suspended particulate matter samples. *Aerosol Sci. Eng.*, 1 (2):193–205.
- Wild, R.J., Dubé, W.P., Aikin, K.C., Eilerman, S.J., Neuman, J. A., Peischl, J., Ryerson, T.B., Brown, S.S. (2017). On-road measurements of vehicle NO<sub>2</sub>/NO<sub>x</sub> emission ratios in Denver, Colorado, USA. *Atmos. Environ.*, 148:182–189.
- Zhang, Y., Wang, X., Li, G., Yang, W., Huang, Z., Zhang, Z., Huang, X., Deng, W., Liu, T., Huang, Z., Zhang, Z. (2015). Emission factors of fine particles, carbonaceous aerosols and traces gases from road vehicles: Recent tests in an urban tunnel in the Pearl River Delta, China. *Atmos. Environ.*, 122:876–884.